and $-2.04\,e\,Å^3$ (SADABS, SHELXS/L by G. M. Sheldrick, Universität Göttingen, Germany, **1993** and **1997**; structural graphics with DIAMOND 2.1 from K. Brandenburg, Crystal Impact GbR, **1999**). Several individual crystals were measured. Further details on the crystal structure investigation may be obtained from the Fachinformationszentrum Karlsruhe, 76344 Eggenstein-Leopoldshafen, Germany (fax: (+49)7247-808-666; e-mail: crysdata@fiz-karlsruhe.de), on quoting the depository number CSD-411939.

[6] I. D. Brown in *Structure and Bonding in Crystals, Vol. II* (Eds.: M. O'Keeffe, A. Navrotsky), Academic Press, New York, **1981**, pp. 1–30.

[7] "ESR Spectra of Metal Complexes of the First Transition Series in Low Symmetry Environments": A. Bencini, D. Gatteschi in *Transition Metal Chemistry, Vol. 8* (Eds.: B. N. Figgis, G. A. Melson), Marcel Dekker, New York, **1982**, pp. 1–178; J. R. Wasson, P. J. Corvan, W. E. Hatfield, *Inorg. Chim. Acta* **1978**, *27*, 167–171.

[8] The generation of giant wheel-based porous materials and the relevant investigation of their catalytic properties is a separate project investigated together with Prof. F. Schüth (MPI, Mühlheim). The material has to be heated to a well-defined temperature, not too low to guarantee the loss of crystal water, and not too high to avoid cluster deposition. The process is not easy because of the high hydrophilicity of the cluster and the possible release of coordinated H_2O.

[9] A. Müller, S. K. Das, H. Bögge, M. Schmidtmann, A. Botar, A. Patrut, *Chem. Commun.* **2001**, 657–658.

[10] This process can formally (!) be correlated with a general symmetry formalism or symmetry-evolution principle for a quasi-isolated system[11] if only the microworld of the molecular intermediates is considered and not the macroscopic system, for which structure-formation-based precipitation is equivalent to symmetry breaking (cf. H. Genz, *Symmetrie—Bauplan der Natur*, Piper, München, **1987**). The important aspect is that the highly symmetrical species are preferably formed as they are kinetically more inert.

[11] J. Rosen, *Symmetry in Science: An Introduction to the General Theory*, Springer, New York, **1995**.

[12] A. Müller, S. K. Das, C. Kuhlmann, H. Bögge, M. Schmidtmann, E. Diemann, E. Krickemeyer, J. Hormes, H. Modrow, M. Schindler, *Chem. Commun.* **2001**, 655–656.

[13] A. Bielanski, A. Malecka-Lubanska, J. Pozniczek, A. Müller, E. Krickemeyer, E. Diemann, *Bull. Pol. Acad. Sci. Chem.* **2001**, *49*, 85–99.

Structure of $Ca_{13}Cd_{76}$: A Novel Approximant to the $MCd_{5.7}$ Quasicrystals (M = Ca, Yb)**

Cesar Pay Gómez* and Sven Lidin

The compound $Ca_{13}Cd_{76}$ has been synthesized and its structure has been solved from single crystal X-ray diffraction data.[1] The discovery of the stable binary icosahedral quasicrystals $YbCd_{5.7}$ and $CaCd_{5.7}$ opens the doors to new possibilities for understanding quasicrystalline structures.[2, 3] A stable quasicrystalline phase has the obvious advantage that large, single-grain crystals can be grown, which allow detailed investigations of physical properties in the bulk, structural studies with neutron radiation, etc. Most stable quasicrystals are ternary or multinary, and this leads to uncertainties in the occupancy of different atomic sites in the structure. A binary quasicrystal thus offers the additional advantage of simplicity in its structural description. The uniqueness of the $MCd_{5.7}$ (M = Ca, Yb) quasicrystals lies in the combination of these features. Although icosahedral approximants are ubiquitous,[4] the $MCd_{5.7}$ compounds are the only known icosahedral quasicrystals that exhibit both these characteristics.

The structures of the quasicrystal approximants play a key role in understanding quasicrystals, since they are expected to display the same local arrangements as the true quasicrystals, and their long-range order facilitates their structural determination by standard methods. Thus, they provide a link to the underlying mechanism of quasicrystal formation.

Modeling quasicrystals is a very attractive way to predict thermodynamic stability, but large multinary approximants containing several different d- or f-block elements do not easily lend themselves to calculations. $Ca_{13}Cd_{76}$ is even better suited in this context; not only is it a well-ordered, binary system with accurately defined sites for the two types of metal atoms, it is for all practical purposes composed of elements with closed-shell cores.

The classic approximants to the $MCd_{5.7}$ quasicrystals are the long known $CaCd_6$ and $RECd_6$ (RE = rare earth metal) phases;[5, 6] recent investigations conducted at our department, however, show that their true structures have yet not been well characterized. The characterization of $Ca_{13}Cd_{76}$ (or $CaCd_{5.85}$) shows that it is a more closely related approximant to the $MCd_{5.7}$ quasicrystals than any other so far known. The relation between the structures of $CaCd_6$, $Ca_{13}Cd_{76}$, and the icosahedral $MCd_{5.7}$ quasicrystals is implicitly evident from the diffraction patterns of the two approximants; the tenfold symmetry of the patterns is clearly enhanced in $Ca_{13}Cd_{76}$ compared to that of $CaCd_6$ (Figure 1). The recurring structural building blocks seen in the $RECd_6$ phases, $CaCd_6$, and the $RE_{13}(Zn,Cd)_{58}$ phases can be found in $Ca_{13}Cd_{76}$, but in a new, spectacular arrangement.[7, 8] A comparison of the Yb–Cd and the Ca–Cd binary phase diagrams reveals that the systems are very similar; several isostructural phases are present. The compounds $CaCd_{5.7}$ and $YbCd_{5.7}$ were earlier reported in these two systems (as Ca_3Cd_{17} and $YbCd_{5.7}$) but in no other.[5, 9] However, their structures had not previously been characterized. Furthermore, a comparison of atomic radii shows that Yb and Ca are almost identical in size; not even the neighboring lanthanides match the size of Yb better than Ca. The atomic size apparently must be restricted to a narrow span to allow the formation of the $CaCd_{5.85}$, $CaCd_{5.7}$, and $YbCd_{5.7}$ phases. This could explain why no other lanthanides form these phases in combination with Cd, though the 1:6 approximants exist in almost all RE–Cd systems. Furthermore, both Yb and Ca have two s electrons in their outer shell and form divalent ions. All these similarities between the elements make Ca the perfect candidate for the formation of a compound that is next of kin to the $MCd_{5.7}$ quasicrystals.

$Ca_{13}Cd_{76}$ crystallizes in the cubic space group $Pa\bar{3}$ (no. 205), with $a = 25.339(2)$ Å. A convenient way to describe the structure is to identify a unique structural building block and then further describe the cell content in terms of the

---

[*] C. P. Gómez, Prof. Dr. S. Lidin
Inorganic Chemistry, Arrhenius Laboratory
Stockholm University, 106 91 Stockholm (Sweden)
Fax: (+46)8-152187
E-mail: cesar@inorg.su.se

[**] This study was financially supported by the Swedish Natural Science Research Council.

1433-7851/01/4021-4037 $ 17.50+.50/0

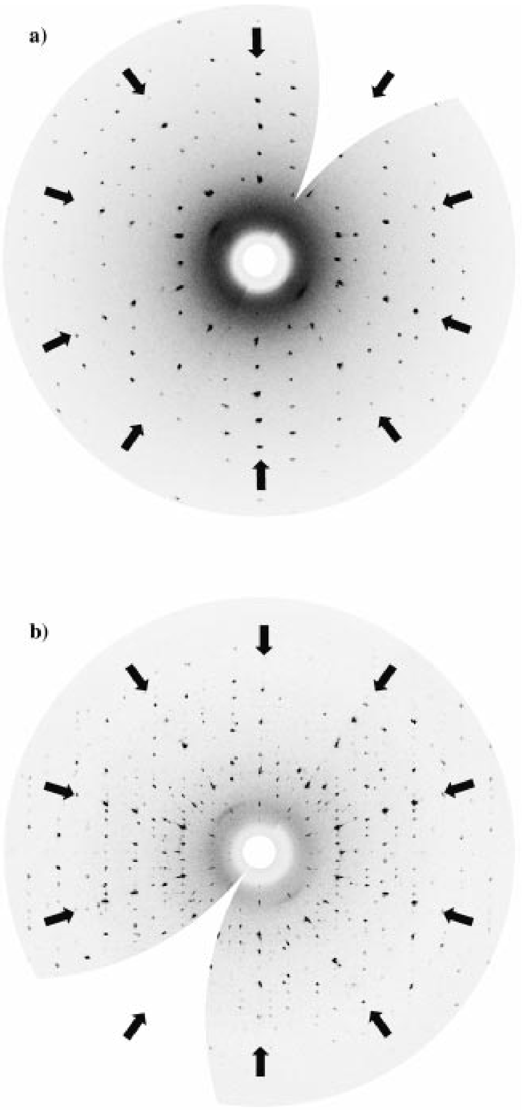

Figure 1. The diffraction pattern of a $RECd_6$ approximant is seen in a) a section through the origin of reciprocal space perpendicular to [850]. The diffraction pattern of $Ca_{13}Cd_{76}$ is seen in b) a section through the origin of reciprocal space, perpendicular to [21 13 0]. The directions were chosen to give a good approximation to the ideal $[\tau 1 0]$, where $\tau = (\sqrt{5}+1)/2$. The strong main reflections exhibit an accentuated tendency to tenfold symmetry in (b). This feature is present but less apparent and has stronger deviations from perfect decagonality in (a). An interesting feature in comparing the cell parameter of $CaCd_6$ with that of $Ca_{13}Cd_{76}$ is that they relate as $1{:}\tau$. The data presented in (b) were collected on a macroscopically twinned crystal.

distribution of such building blocks. The central core of the basic building block consists, in analogy with $CaCd_6$ and the $RECd_6$ phases, of a Cd_{20} pentagonal dodecahedron that encloses a disordered Cd_4 tetrahedron.

The Cd atoms are arranged in two ways around the Ca atoms. The first is a monocapped, double pentagonal antiprism ($CaCd_{16}$ polyhedron; Figure 2a), an arrangement that is known from Ce_6Cd_{37}, $CaCd_6$, the $RECd_6$ and $RE_{13}(Zn,Cd)_{58}$ phases.[10] The second arrangement is a double Friauf polyhedron (Figure 2b), which is known from several other intermetallic compounds.[11] The construction of the basic building block from $CaCd_{16}$ polyhedra, Cd_8 cubes, and double Friauf polyhedra is illustrated in Figure 3. The presence of Cd_8 cubes is not unique to $Ca_{13}Cd_{76}$; once again the kinship to the $RECd_6$ and $RE_{13}(Zn,Cd)_{58}$ phases is apparent. In $Ca_{13}Cd_{76}$ all cubic interstices are vacant.

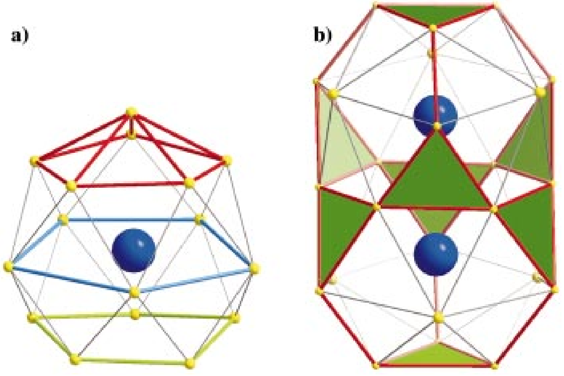

Figure 2. The different arrangements of Cd atoms (yellow) around Ca atoms (blue) in $Ca_{13}Cd_{76}$. a) The $CaCd_{16}$ polyhedron, a monocapped double pentagonal antiprism. b) The double Friauf polyhedron, two truncated tetrahedra sharing a hexagonal face. All hexagonal faces are capped by Cd atoms, except for the shared face, in which the Ca atoms mutually serve as capping atoms for one another.

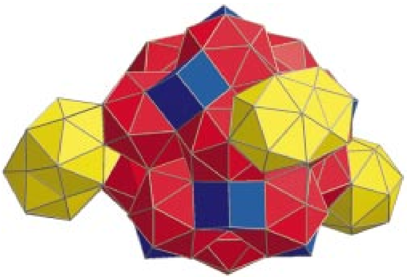

Figure 3. Polyhedral model of the basic building block in $Ca_{13}Cd_{76}$. The $CaCd_{16}$ polyhedra (red), the three surrounding double Friauf polyhedra (yellow), and the vacant Cd_8 cubes (blue) have been combined to construct the building block. Cd atoms are the corners of all polyhedra in the figure.

An alternative way of constructing the basic building block is displayed in Figure 4. This representation is preferable for describing the structures of $Ca_{13}Cd_{76}$ and $CaCd_6$ as the simple packings of triacontahedral clusters seen in Figure 5a and b. The main difference between the structure of $Ca_{13}Cd_{76}$ and that of the closely related compound $CaCd_6$ is the packing of the triacontahedra. The triacontahedron is not a space-filling polyhedron, and in $Ca_{13}Cd_{76}$ this problem is solved by interpenetration of the triacontahedral clusters and by the creation of cavities. Two Ca atoms are fitted into each of these cavities to form the double Friauf polyhedron (Figure 6). In $CaCd_6$ the problem of space filling is solved solely by interpenetration of the triacontahedra.

The unforeseen introduction of a double Friauf polyhedron allows for new ways to arrange the triacontahedral clusters; this knowledge could prove useful in modeling the structures of the $MCd_{5.7}$ quasicrystals.

Experimental Section

Crystals of $Ca_{13}Cd_{76}$ were obtained by placing a mixture of Cd metal (1.0101 g; splinters from a rod of pure metal, purified by melting) and Ca (0.0736 g; STREM 99.9 %) in a steel ampoule that was sealed under argon atmosphere. The sample was first preheated in a high-frequency induction furnace (two 5-s bursts, well above 1300 K). The ampoule was then inserted into a regular furnace for 1 min at 1133 K, quenched to ambient temper-

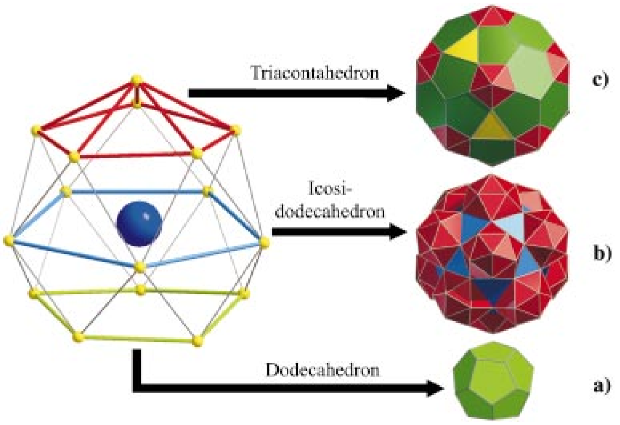

Figure 4. Spherical representation of the basic building block. The spherical layers are created by interconnecting the different pentagonal planes of the $CaCd_{16}$ polyhedra. To emphasize this and the relation with the polyhedral model in Figure 3, the $CaCd_{16}$ polyhedra are included in (b) and (c). Interconnection of the basal pentagonal planes (green) yields the pentagonal dodecahedron in (a); it is somewhat distorted by the disordered Cd_4 tetrahedron residing inside. Interconnection of the intermediate pentagonal planes (blue) gives an icosidodecahedron, a polyhedron composed entirely of equilateral triangles and regular pentagons, shown in blue in (b). The outermost shell of the basic building block is generated by connecting the pentagonal pyramids (red) through the equidistant Cd atoms located in between. This results in a defect rhombic triacontahedron (c). A few of the corner atoms are missing; this is represented by two yellow triangular faces in (c). These vacant positions correspond to positions inside the Cd_8 cubes in Figure 3. Occupation of the cubic interstices by Cd atoms would yield the complete triacontahedron. Occupied and vacant Cd_8 cubes have been observed before in Ce_6Cd_{37}, $Dy_{13}Zn_{57}$, and several other $RECd_6$ and $RE_{13}(Zn,Cd)_{58}$ phases.[7] However, the single-crystal data collected for $Ca_{13}Cd_{76}$ do not support a structure with filled cubic interstices.

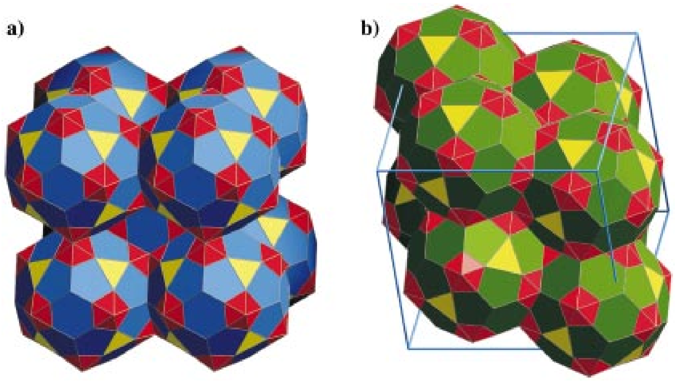

Figure 5. The structure of $CaCd_6$ (a) can be described as a body-centered cubic arrangement of partially interpenetrating triacontahedra. The cell content of $Ca_{13}Cd_{76}$ (b) can similarly be described as a cubic close-packed arrangement of partially interpenetrating triacontahedra. The yellow triangles indicate missing corner atoms.

ature, reinserted at 858 K, and held at that temperature for 90 h. The furnace was then turned off, and the sample was left inside to cool down to ambient temperature (cooling rate ca. 3° min^{-1}).

The diffraction data were collected on a STOE IPDS single-crystal X-ray diffractometer with a rotating-anode $Mo_{K\alpha}$ X-ray source, and the determination of the structure by direct methods was performed with the program SHELXS-86.[12] The refinement of the structure was performed on a twinned crystal by using the program JANA98.[13] The intensities of the reflections were integrated with the STOE software, and the numerical absorption correction was performed with the programs X-RED and X-SHAPE.[14]

Received: April 19, 2001
Revised: July 16, 2001 [Z16966]

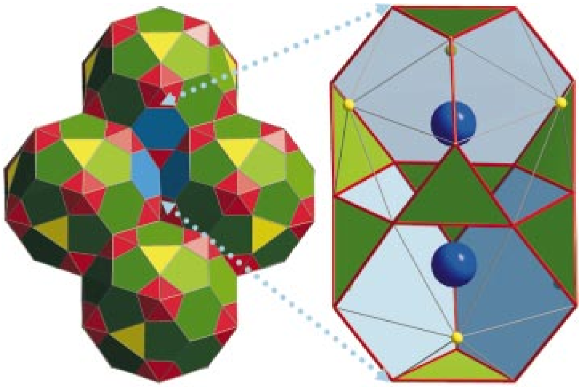

Figure 6. The double Friauf polyhedron is located at the junction where eight of the triacontahedral clusters meet. Four of these clusters have been removed in the figure, and the hexagonal faces of the double Friauf polyhedron are highlighted in blue for clarity.

[1] Crystallographic data for $Ca_{13}Cd_{76}$: $M_r = 9063.4$, cubic, space group $Pa\bar{3}$ (no. 205), $a = 25.339(2)$ Å, $V = 16270(1)$ Å^3, $Z = 8$, $\rho_{calcd} = 7.401$ $g\,cm^{-3}$, $F(000) = 31226$, $\mu(Mo_{K\alpha}) = 20.19$ mm^{-1}, crystal dimensions $0.3 \times 0.27 \times 0.25$ mm. Diffraction data were collected on a STOE IPDS at 298 K; $2\theta = 3.9-51.9°$, 5242 independent reflections, 1965 observed reflections ($I > 3\sigma(I)$), $R_{int}(obs/all) = 0.109/0.139$, 258 parameters, $R(F) = 0.0525$, $R_w(F) = 0.0496$, numerical absorption correction from X-SHAPE, $T_{min}/T_{max} = 0.0301/0.0737$, $\Delta\rho_{min}/\Delta\rho_{max} = 4.985/-3.912$ e Å^{-3}, Δ/e.s.d = 0.0004. Further details on the crystal structure investigations may be obtained from the Fachinformationszentrum Karlsruhe, 76344 Eggenstein-Leopoldshafen, Germany (fax: (+49) 7247-808-666; e-mail: crysdata@fiz-karlsruhe.de), on quoting the depository number CSD-411887.

[2] A. P. Tsai, J. Q. Guo, E. Abe, H. Takakura, T. J. Sato, *Nature* **2000**, *408*, 537–538.
[3] J. Q. Guo, A. P. Tsai, E. Abe, *Phys. Rev. B* **2000**, *62*, R14605–R14608.
[4] D. P. Shoemaker, C. B. Shoemaker in *Introduction to Quasicrystals* (Ed.: M. V. Jarić), Academic Press, San Diego, **1988**, chap. 1, pp. 1–52.
[5] G. Bruzzone, *Gazz. Chim. Ital.* **1972**, *102*, 234–242.
[6] E. Ryba, P. K. Kejriwal, R. Elmendorf, *J. Less-Common Met.* **1969**, *18*, 419–422.
[7] C. P. Gómez, S. Lidin, *Solid State Sci.*, in press.
[8] G. Bruzzone, M. L. Fornasini, F. Merlo, *J. Less-Common Met.* **1973**, *30*, 361–375.
[9] A. Palenzona, *J. Less-Common Met.* **1971**, *25*, 367–372.
[10] M. Armbrüster, S. Lidin, *J. Alloy. Compd.* **2000**, *307*, 141–148.
[11] F. Laves, H. Witte, *Metallwirtsch. Metallwiss. Metalltech.* **1935**, *14*, 645–649.
[12] G. M. Sheldrick, University of Göttingen, Göttingen, Germany, **1990**.
[13] V. Petíek, M. Dušek, Institute of Physics AVCR, Praha, Czech Republic, **1997**.
[14] STOE & Cie GmbH, Darmstadt, Germany, **1996**, v. 1.07.